

Shape Restoration Effect in Ag–SiO₂ Core–Shell Nanowires

Sergei Vlassov,^{*,†} Boris Polyakov,[†] Leonid M. Dorogin,^{‡,§} Mikk Vahtrus,[‡] Magnus Mets,[‡] Mikk Antsov,^{‡,§} Rando Saar,[‡] Alexey E. Romanov,^{‡,||,⊥} Ants Lõhmus,[‡] and Rünno Lõhmus^{‡,§}

[†]Institute of Solid State Physics, University of Latvia, Kengaraga 8, LV-1063, Riga, Latvia

[‡]Institute of Physics, University of Tartu, Riia 142, 51014, Tartu, Estonia

[§]Estonian Nanotechnology Competence Centre, Riia 142, 51014, Tartu, Estonia

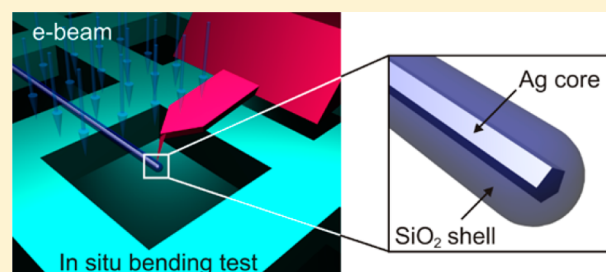
^{||}ITMO University, Kronverkskiy pr., 49, 197101 St. Petersburg, Russia

[⊥]Ioffe Physical Technical Institute, RAS, Politehnicheskaja st. 26, 194021 St. Petersburg, Russia

S Supporting Information

ABSTRACT: The combination of two different materials in a single composite core–shell heterostructure can lead to improved or even completely novel properties. In this work we demonstrate the enhancement of the mechanical properties of silver (Ag) nanowires (NW) achieved by coating them with a silica (SiO₂) shell. In situ scanning electron microscope (SEM) nanomechanical tests of Ag–SiO₂ core–shell nanowires reveal an improved fracture resistance and an electron-beam induced shape restoration effect. In addition, control experiments are conducted separately on uncoated Ag NWs and on empty SiO₂ shells in order to gain deeper insight into the peculiar properties of Ag–SiO₂. Test conditions are simulated using finite-element methods; possible mechanisms responsible for the shape restoration and the enhanced fracture resistance are discussed.

KEYWORDS: Core–shell nanowires, mechanical properties, shape restoration, electron beam, scanning electron microscopy



Silver nanowires (Ag NWs) are a promising material for nanoscale systems due to their excellent electrical and thermal conductivity,^{1,2} perfect structure, and ease of synthesis. Among other applications, Ag NWs are considered as an alternative and even replacement to indium tin oxide (ITO) in making transparent, flexible, and conductive films.^{3–6} Ag NWs can also serve as waveguides for plasmon propagation in nanophotonics.⁷ In many applications, NWs are subjected to mechanical stresses. In flexible coatings,^{4,5} as well as in nanorelays, nanoswitches,⁸ and nanoresonators,⁹ NWs must be able to withstand numerous repetitive deformations. In nanophotonics, a significant degree of bending is often required in order to guide the light in the desired direction.¹⁰ It has also been shown that defects or discontinuities—such as cracks introduced by bending of Ag NWs—strongly affect the light propagation in waveguides.^{7,11} Therefore, the improvement of mechanical properties is essential for performance and reliability in the applications described above.

Several works report enhanced elasticity^{12,13} and fatigue resistance of Ag NWs in comparison to bulk silver,¹⁴ which makes them potentially suitable for nano- and micro-electromechanical systems (NEMS and MEMS) applications. A serious drawback of Ag NWs is aging, which leads to the deterioration of these attractive properties. Aging could be inhibited by coating Ag NWs with protective layers like SiO₂^{15–18} or TiO₂¹⁹ via a relatively simple sol–gel process.²⁰ The coating can be partly removed from the ends of the NWs in order to form nanocables and to serve as interconnects in

nanoscale electronic circuits. Moreover, it has been demonstrated that coating can also enhance the optical properties of metallic NWs.^{21,22} Therefore, the engineering of one-dimensional (1D) core–shell heterostructures opens a new route for creation of novel materials with advanced properties.

In spite of their attractive optical properties and rich potential, the mechanical properties of 1D core–shell nanostructures are still poorly studied. Several theoretical works are available. Aifantis et al. applied a continuum mechanics approach to the modeling of metallic NWs with oxide shells and demonstrated that the presence of the interface between the core and the shell influences significantly the overall mechanical response of a NW during loading.²³ Liu et al. studied the composition-dependent Young's modulus for Ge-core/Si-shell and Si-core/Ge-shell NWs and found a nonlinear dependence of Young's modulus on the Si/Ge composition ratio.²⁴ To the best of our knowledge, no experimental works are available on the mechanical properties of core–shell NWs. The goal of this paper is to demonstrate the remarkable mechanical properties of 1D Ag–SiO₂ heterostructures and to encourage the usage of core–shell NWs in various MEMS and NEMS applications.

Received: May 22, 2014

Revised: August 21, 2014

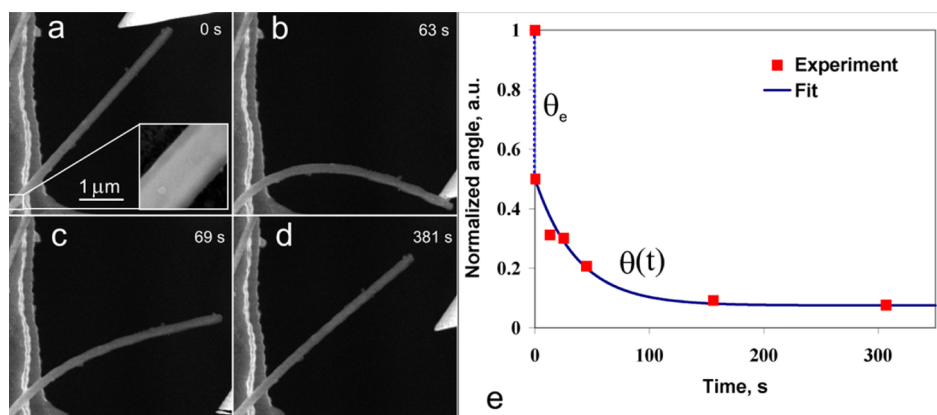


Figure 1. Shape-restoration effect of a core-shell Ag-SiO₂ NW. Tip approaches a NW (a). NW is gradually bent to a curvature 0.66 μm⁻¹ and held in a bent state approximately 1 min (b). Tip retracted from NW and it starts to straighten (c). NW restored almost to its initial straight shape (d). Corresponding plot of the normalized restoration angle versus time (e). The degree of shape restoration for this particular experiment is 92%. The relaxation time is 26 s. The inset shows the core-shell structure of NW (enhanced contrast). SEM parameters: acceleration voltage 10 kV, probe current 0.34 pA.

Ag-SiO₂ core-shell NWs were produced by coating silver NWs (BlueNano, Charlotte, NC, USA) with SiO₂ shell according to a well-established sol-gel method.^{15,21,22} Intact Ag NWs had a smooth, uniform, 5-fold-twinned crystalline structure.¹⁴ Diameters ranged from tens to a few hundred nanometers and lengths on the order of several to tens of μm. Two sets of core-shell structures were created: one with the SiO₂ shell thickness of approximately 34 ± 6 nm (set 1, “thick-shelled”) and 10 ± 5 nm (set 2, “thin-shelled”) (see the Supporting Information, Figure S1). The resulting NWs were characterized with a high-resolution scanning-electron microscope (HRSEM; FEI Helios Nanolab 600) equipped with an X-ray diffractometer (XRD; Oxford Instruments, UK). In order to study the properties of the SiO₂ shells separately, empty tubes were made by etching the core-shell NWs in 50% volume ratio nitric acid (HNO₃) solution for 3 h. A control sample was left in nitric acid for one month in order to make sure that SiO₂ shells do not deteriorate in acid.

An in situ SEM cantilevered beam bending scheme^{25,26} was utilized in order to investigate the response of individual Ag-SiO₂ NWs, intact Ag NWs, and empty SiO₂ tubes to external loading. Test samples of core-shell NWs and intact Ag NWs were prepared by depositing the NWs onto transmission-electron microscope (TEM) square-mesh grids (Agar, UK) from methanol and ethanol, respectively. SiO₂ tubes were deposited from HNO₃ solution to a silicon calibration grating (TGXYZ03, Mikromasch, NanoWorld Holding AG, Switzerland). Measurements were performed inside the HRSEM and consisted in visually controllable gradual bending of single half-suspended NWs by the atomic-force microscope (AFM) tip (ATEC-CONT cantilevers, Nanosensor, Neuchatel, Switzerland, C = 0.2 N m⁻¹) attached to a micromanipulator (MM3A-EM, Kleindiek, Germany). Nanoindentation of empty SiO₂ tubes was done by AFM (Dimension Edge, Veeco) at ambient conditions using tapping-mode cantilevers (PPP-NCH, Nanosensors).

In bending tests of “thick-shelled” Ag-SiO₂ NWs it was found that, after removal of the external force, the bent NWs restored to their initial profile within minutes (Figure 1). The effect was found to be electron-beam activated. When the electron beam was switched off, shape restoration ceased, and the NW profile was “frozen”. As soon as the beam was switched

on again, the shape restoration resumed from the last profile. Previously bent and restored NWs were bent again multiple times, and every time shape restoration was observed.

Dynamics of the shape restoration (Figure 1e) resembled the behavior of viscoelastic materials.²⁷ Restoration started from rapid elastic straightening followed by slow viscoelastic relaxation naturally approximated by an exponential fit: $\theta(t) = (1 - \theta_e - \theta_0)\exp[-t/\tau] + \theta_0$, where θ is the total normalized angle, θ_e is the contribution of elastic restoration, θ_0 is the residual angle due to plastic deformation, and τ is the characteristic relaxation time.

In total, nine Ag-SiO₂ NWs were investigated, and it was found that complete shape restoration takes place for bending curvatures up to approximately 0.4 μm⁻¹ (Table S1 in Supporting Information). The effect of restoration was also observed for larger bending curvatures; however, the initial straight profile was not reached due to residual plastic deformation.

In addition to shape restoration effect, Ag-SiO₂ NWs demonstrated high fracture resistance and withstood severe deformation without visible fracture. For most Ag-SiO₂ NWs, it was possible to bend them into a loop with curvature exceeding 2.1 μm⁻¹ (Figure 2) without visible signs of fracture, in contrast to uncoated Ag NWs, which often break in a brittle-like manner in a bending test as was shown by Vlassov et al.¹⁴ It was demonstrated that uncoated Ag NWs exhibited significant elasticity, allowing pure elastic bending before critical curvature reached, followed either by plastic deformation (critical curvature 0.8 μm⁻¹) for 2/3 of all tested NWs or by brittle-like fracture (critical curvature 1.66 μm⁻¹) for remaining 1/3 of NWs. A typical Ag NW bending experiment is shown in Figure S2 in Supporting Information. In very few cases Ag-SiO₂ NWs also broke in bending test due to brittle-like fracture of silica shell (see Figure S3 in the Supporting Information for broken uncoated Ag NW and Ag-SiO₂ NW).

Let us estimate the stresses generated in the silver core during a bending test of Ag-SiO₂ NWs. Elastic deformation of the silver core enables consideration of bending strain in the framework of the elastic beam model (see, e.g., ref 28). Maximal mechanical stress σ in the bent NW core can be found according to the relation $\sigma = Er\kappa$,^{29,30} where E is Young’s modulus (83 GPa for Ag³¹), r is the radius of the Ag core, and κ

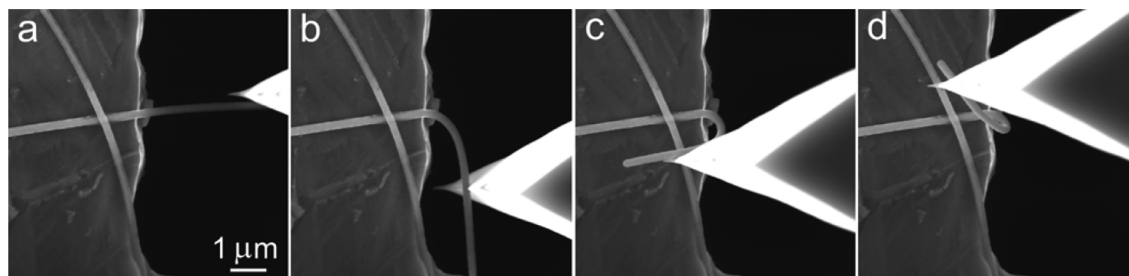


Figure 2. Series of images from bending test of “thick-shelled” Ag–SiO₂ NW (core radius $r = 80$ nm, shell thickness 32 nm). NW is gradually bent to a curvature $1.28 \mu\text{m}^{-1}$ (b), $2.1 \mu\text{m}^{-1}$ (c), and more (d) without visible fracturing.

is the maximum bending curvature. The maximal stress in the Ag core after which complete shape restoration was observed is 3.3 GPa (see Supporting Information, Table S1). Overall, in bending experiments the stresses in the core of core–shell NWs exceeded 10 (up to 15) GPa without visible fracture, while uncoated Ag NWs start to fracture at stress of 8.5 GPa. However, we cannot exclude appearance of structural defects in the Ag core of core–shell NWs during severe deformations (an additional study in TEM is needed to reveal internal defects in the Ag core).

To investigate the resistance of Ag–SiO₂ NWs to repeated loads, a fatigue test was performed consisting of one million bending cycles applied to a single core–shell NW over 16 min. The amplitude of the bending load was chosen in order to ensure complete shape restoration according to Table S1. No signs of fracture were observed neither in the core nor in the shell. The initial straight profile was completely restored after removal of the external force.

In order to get deeper insight into the properties of Ag–SiO₂ heterostructures, and the reasons for shape restoration and enhanced fracture resistance, additional bending experiments were performed in similar conditions on empty SiO₂ nanotubes (NT) and Ag–SiO₂ NWs with thinner shells.

Empty SiO₂ NTs demonstrated high fracture resistance similar to that of Ag–SiO₂ NWs. NTs were routinely bent without any visible fracture achieving curvature up to $3.25 \mu\text{m}^{-1}$. An apparent time-dependent response to mechanical load was revealed. Elastic behavior was noticed for higher bending rates (time scale of a few seconds), while lower bending rates (tens of seconds and more) led to residual deformation. No signs of shape restoration—even after up to 17 min of e-beam irradiation in SEM—were observed (see the Supporting Information, Figure S4). The observed viscoelastic transition can be explained by nonthermal electron-beam induced structural relaxation in bent SiO₂ NTs via creation and increased mobility of defects, as was recently demonstrated by Zheng et al. for nanoscale silica inside TEM.³²

“Thin-shelled” Ag–SiO₂ NWs demonstrated no considerable fracture resistance or shape restoration in bending experiments. In general, the behavior was similar to uncoated Ag NWs. From this it can be concluded that the peculiar properties of Ag–SiO₂ core–shell NWs strongly depend on the thickness of SiO₂ shell.

Taking into account the properties of uncoated Ag NWs and empty SiO₂ shells, the overall response of Ag–SiO₂ NW system to bending deformation should be determined by an interplay between the elasticity of the core and the e-beam induced viscosity of the shell. We propose that bent core–shell NWs are restored back to the initial straight shape by an elastic driving force in the core against the viscously resisting shell. The explanation of a viscoelastic flow is supported by the fact that

the type of deformation of core–shell NWs under electron-beam irradiation was strongly dependent on deformation rate. Rapidly (on the time scale of few seconds) deformed and immediately released core–shell NWs exhibited purely elastic behavior. At slower deformation rates (tens of seconds and more), NWs behaved like viscous materials, and slow shape restoration was observed.

In addition to experimental measurements, bending test conditions were simulated using a finite-elements method (FEM, COMSOL Multiphysics 4.4) to estimate the e-beam induced viscosity of the shell and illustrate the distribution of mechanical stresses in the vicinity of the NW part rigidly fixed to the substrate. Based on the SEM images of individual Ag and Ag–SiO₂ NWs, the geometry of the system was set to the prismatic rod with a circular outer and pentagonal cross-section at the interface. The core was modeled as elastic material with Young’s modulus of the silver (83 GPa). Shell was divided into two domains consisting from viscous and elastic parts (see Supporting Information, Figure S5) in order to account for the fact that in experiment lower part of the shell is shielded from e-beam by the silver core and therefore should remain purely elastic. The Young’s modulus of the elastic part of the shell (25 GPa) was measured in a standard AFM nanoindentation test. Parameters of inner and outer radii, NW length, and deflection were taken from real experiments. The modeled composite beam was firmly fixed from one end, while the other end was deformed by a point force followed by releasing and viscoelastic relaxation of the NW. The viscosity η of the shell was varied to find proper fit between experimental and simulated relaxation curves. Extracted η values (from 2×10^{11} to 2×10^{12} Pa·s/ 7×10^{11} Pa·s in average) were found to be very close to glass transition viscosity of solids according to widely accepted definition,³³ from which it can be concluded that the e-beam is capable to cause glass transition in SiO₂ subjected to an external load.

A similar simulation was performed to illustrate the distribution of mechanical stresses in the vicinity of the NW part rigidly fixed to the substrate. For uncovered Ag NW von Mises stresses are concentrated at the interface between the adhered and suspended parts and can easily exceed the strength of Ag, being therefore the most probable region for plastic yield and fracture (see Supporting Information, Figure S6). When the SiO₂ layer is present, the stresses are mainly concentrated in the shell and relieved in the Ag core (Figure 3). For simplicity, the upper part of the shell, exposed to e-beam in real experiment, was removed from the simulations. The consideration above allows for the investigation of the damping role of the shell in the bending tests, the protection of the Ag core from plastic yield, and crack formation.

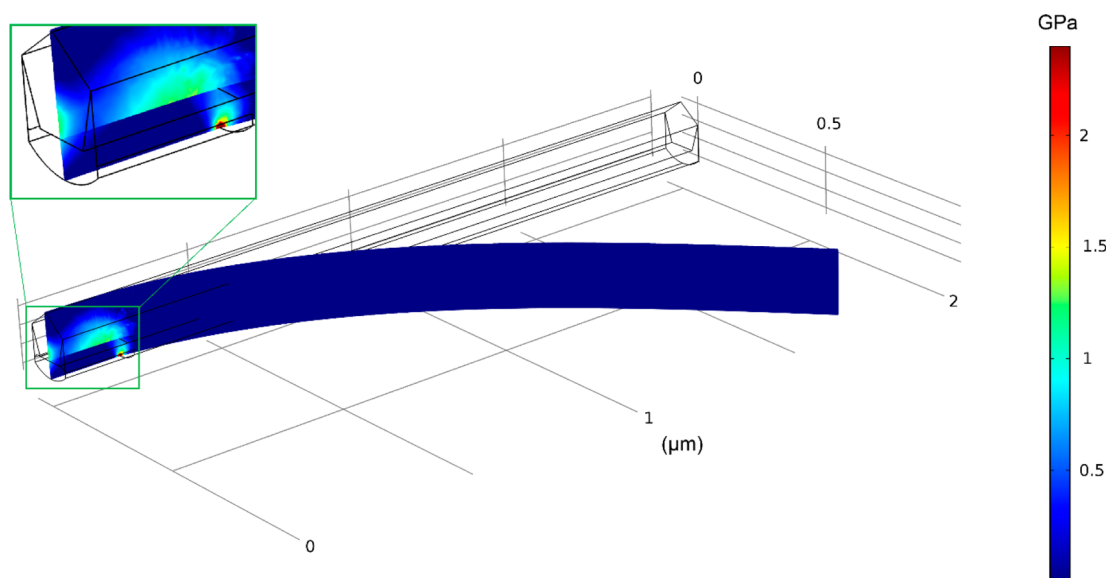


Figure 3. Distribution of von Mises stress in the vicinity of the fixed part of a bent Ag NW with interlaid elastic SiO₂ layer (COMSOL Multiphysics).

The role of shell might also extend to the prevention of the nucleation of defects at the core–shell interface and intrinsic structural transformations. One example of a possible transformation in pentagonal Ag NWs is kinking or twinning observed in ref 34 as a result of bending. Mitigation of this kind of deformation can be related to the presence of an amorphous shell, although more detailed theoretical and experimental investigation has to be carried out to justify this effect.

In conclusion, we performed half-suspended beam-bending tests on Ag–SiO₂ core–shell nanowires and demonstrated enhanced fracture resistance and electron beam promoted shape restoration effects. Shape restoration was shown to be a phenomenon exclusively inherent to core–shell heterostructures, and absent for pure Ag NWs or SiO₂ shells separately. Shape restoration was explained as e-beam induced structural relaxation of the SiO₂ shell governed by elastic forces generated by the deformed Ag core. Test conditions were simulated using FEM, and the average value of e-beam induced viscosity of the shell $\eta = 7 \times 10^{11}$ Pa·s was extracted by fitting simulated relaxation curves with experimental data. The stresses in the core of core–shell NWs in bending experiments can reach to 15 GPa without visible fracture, in contrast to uncoated Ag NWs, which start to fracture at a stress of 8.5 GPa. According to finite element method simulations, the shell can dampen the mechanical stresses in the core in the vicinity of the contact with a stiff substrate and mitigate the plastic yield in the core. To the best of our knowledge, this is the first experimental work on the mechanical characterization of metal–oxide core–shell NWs. The reported results clearly demonstrate that the combination of two different materials in composite core–shell heterostructures can lead to materials with advanced properties.

■ ASSOCIATED CONTENT

📄 Supporting Information

SEM micrograph of a core–shell Ag–SiO₂ NWs; statistics of shape restoration of Ag–SiO₂ NWs; results of fatigue test; bending of pure an Ag NW; fracture of uncoated Ag NW and core–shell NW; bending of SiO₂ nanotube (Ag core etched off chemically). This material is available free of charge via the Internet at <http://pubs.acs.org>.

■ AUTHOR INFORMATION

Corresponding Author

*E-mail address: vlassovs@ut.ee.

Notes

The authors declare no competing financial interest.

■ ACKNOWLEDGMENTS

This work was supported by EU ERDF project Centre of Excellence “Mesosystems: Theory and Applications”, TK114. The work was also partly supported by the ESF project no. 2013/0015/1DP/1.1.1.2.0/13/APIA/VIAA/010, IUT2-25, ETF grants 8420, 9007, Estonian Nanotechnology Competence Centre (EU29996), ERDF “TRIBOFILM” 3.2.1101.12-0028, “IRGLASS” 3.2.1101.12-0027, and “Nano-Com” 3.2.1101.12-0010. The support from ITMO International Research Laboratory Program is acknowledged.

■ REFERENCES

- (1) Wiley, B.; Sun, Y.; Xia, Y. *Acc. Chem. Res.* **2007**, *40* (10), 1067–1076.
- (2) Caswell, K. K.; Bender, C. M.; Murphy, C. J. *Nano Lett.* **2003**, *3* (5), 667–669.
- (3) Liu, C.-H.; Yu, X. *Nanoscale Res. Lett.* **2011**, *6*, 75.
- (4) Lee, P.; Lee, J.; Lee, H.; Yeo, J.; Hong, S.; Nam, K. H.; Lee, D.; Lee, S. S.; Ko, S. H. *Adv. Mater.* **2012**, *24* (25), 3326–3332.
- (5) Lee, J.; Lee, P.; Lee, H.; Lee, D.; Lee, S. S.; Ko, S. H. *Nanoscale* **2012**, *4*, 6408–6414.
- (6) Lee, J. H.; Lee, P.; Lee, D.; Lee, S. S.; Ko, S. H. *Cryst. Growth Des.* **2012**, *12* (11), 5598–5605.
- (7) Wang, W.; Yang, Q.; Fan, F.; Xu, H.; Wang, Z. L. *Nano Lett.* **2011**, *11* (4), 1603–1608.
- (8) Loh, O. Y.; Espinosa, H. D. *Nat. Nanotechnol.* **2012**, *7* (5), 283–295.
- (9) Li, M.; Bhiladvala, R. B.; Morrow, T. J.; Sioss, J. A.; Lew, K.-K.; Redwing, J. M.; Keating, C. D.; Mayer, T. S. *Nat. Nanotechnol.* **2008**, *3* (2), 88–92.
- (10) Singh, D.; Raghuwanshi, M.; Pavan Kumar, G. V. *Appl. Phys. Lett.* **2012**, *101*, 111111.
- (11) Park, H. S.; Qian, X. J. *Phys. Chem. C* **2010**, *114* (19), 8741–8748.
- (12) Wu, B.; Heidelberg, A.; Boland, J. J.; Sader, J. E.; Sun, X.; Li, Y. *Nano Lett.* **2006**, *6* (3), 468–472.

- (13) Zhu, Y.; Qin, Q.; Xu, F.; Fan, F.; Ding, Y.; Zhang, T.; Wiley, B. J.; Wang, Z. L. *Phys. Rev. B* **2012**, *85*, 045443.
- (14) Vlassov, S.; Polyakov, B.; Dorogin, L. M.; Antsov, M.; Mets, M.; Umalas, M.; Saar, R.; Löhmus, R.; Kink, I. *Mater. Chem. Phys.* **2014**, *143* (3), 1026–1031.
- (15) Yin, Y.; Lu, Y.; Sun, Y.; Xia, Y. *Nano Lett.* **2002**, *2* (4), 427–430.
- (16) Hunyadi, S. E.; Murphy, C. J. *J. Phys. Chem. B* **2006**, *110* (14), 7226–7231.
- (17) Siooss, J. A.; Stoermer, R. L.; Sha, M. Y.; Keating, C. D. *Langmuir* **2007**, *23* (22), 11334–11341.
- (18) Gutierrez-Wing, C.; Perez-Hernandez, R.; Mondragon-Galicia, G.; Villa-Sanchez, G.; Fernandez-Garcia, M. E.; Arenas-Alatorre, J.; Mendoza-Anaya, D. *Solid State Sci.* **2009**, *11* (9), 1722–1729.
- (19) Guo, Y.-G.; Wan, L.-J.; Bai, C.-L. *J. Phys. Chem. B* **2003**, *107* (23), 5441–5444.
- (20) Ramasamy, P.; Seo, D.-M.; Kim, S.-H.; Kim, J. *J. Mater. Chem.* **2012**, *22*, 11651–11657.
- (21) Khanal, B. P.; Pandey, A.; Li, L.; Lin, Q.; Bae, W. K.; Luo, H.; Klimov, V. I.; Pietryga, J. M. *Nano* **2012**, *6* (5), 3832–3840.
- (22) Sun, Y. *Nanoscale* **2010**, *2*, 1626–1642.
- (23) Aifantis, K. E.; Kolesnikova, A. L.; Romanov, A. E. *Philos. Mag.* **2007**, *87* (30), 4731–4757.
- (24) Liu, X. W.; Hu, J.; Pan, B. C. *Physica E* **2008**, *40* (10), 3042–3048.
- (25) Silva, E. C. C. M.; Tong, L.; Yip, S.; Van Vliet, K. J. *Small* **2006**, *2* (2), 239–243.
- (26) Polyakov, P.; Dorogin, L. M.; Vlassov, S.; Kink, I.; Löhmus, A.; Romanov, A. E.; Löhmus, R. *Solid State Commun.* **2011**, *151* (18), 1244–1247.
- (27) Van der Vegt, A. K. *From Polymers to Plastics*; VSSD: Delft, 2002.
- (28) Timoshenko, S.; Goodier, J. N. *Theory of Elasticity*, 2; McGraw-Hill Book Company: New York, 1951; pp 316–342.
- (29) Smith, D. A.; Holmberg, V. C.; Korgel, B. A. *ACS Nano* **2010**, *4* (4), 2356–2362.
- (30) Dorogin, L. M.; Vlassov, S.; Polyakov, B.; Antsov, M.; Löhmus, R.; Kink, I.; Romanov, A. E. *Phys. Status Solidi B* **2013**, *250* (2), 305–317.
- (31) Smith, D. R.; Fickett, F. R. *J. Res. Natl. Inst. Stand. Technol.* **1995**, *100* (2), 119–171.
- (32) Zheng, K.; Wang, C.; Cheng, Y.-Q.; Yue, Y.; Han, X.; Zhang, Z.; Shan, Z.; Mao, S. X.; Ye, M.; Yin, Y.; Ma, E. *Nature Commun.* **2010**, *1*, 24.
- (33) Cusack, N. E. *The Physics of Structurally Disordered Matter*; Adam Hilger: Bristol, 1987.
- (34) Peng, P.; Liu, L.; Gerlich, A. P.; Hu, A.; Zhou, Y. N. *Part. Part. Syst. Charact.* **2013**, *30*, 420–426.